Larmor waves in single-crystal copper at 80 GHz

A. T. Wijeratne and G. L. Dunifer
Department of Physics and Astronomy, Wayne State University, Detroit, Michigan 48202
(Received 4 August 1989)

Larmor waves have been studied using a transmission technique in thin plates of high-purity, single-crystal copper at a frequency of 80 GHz. Observations were made over the temperature range 4–25 K in magnetic fields 0–60 kG with the principal axes ⟨100⟩, ⟨110⟩, or ⟨111⟩ oriented perpendicular to the plane of the specimen. In contrast to earlier observations at 9 GHz, the present studies find a Larmor-wave period which is temperature dependent, and, at the lowest temperatures for certain orientations, an asymmetry in amplitude, with the Larmor-wave oscillations on the high-field side of the conduction-electron-spin resonance being considerably stronger than those on the low-field side. This behavior is not in complete agreement with present theory and may be due to a combination of many-body effects and the detailed geometry of the Fermi surface of copper.

I. INTRODUCTION

Larmor-wave signals have been studied in thin plates of high-purity, single-crystal copper (Cu) using a microwave frequency of 80 GHz. Larmor waves were discovered in the metals Cu and gold by Janossy and Monod[1] in 1976. The signals are observed in microwave transmission experiments carried out at cryogenic temperatures in the presence of a dc magnetic field. The metallic sample, in the form of a thin plate, makes up a common wall between two microwave cavities tuned to the same frequency. Microwaves are introduced into one cavity, the transmit cavity, where they excite the conduction electrons on one surface of the sample. The other cavity, the receive cavity, acts as a receiving antenna picking up any microwave power carried across the sample by the conduction electrons.[2] Under the conditions of low temperature and high magnetic field, the conduction electrons in a pure metal will have $\omega_c\tau \gg 1$, where ω_c is the cyclotron frequency of the electrons and τ is the average momentum scattering time. Under these conditions there exists a large number of modes by which the electrons can be excited and transport energy across the sample. These include modes associated with the electrons' orbital motion[2] and modes associated with spin precession, such as conduction-electron-spin resonance[3] (CESR) and paramagnetic spin waves.[4]

Larmor waves are another mode by which electron spins carry energy across the sample. They are single-particle excitations and results from a small fraction of the electrons on the Fermi surface. This is in contrast to the spin-wave modes which are collective waves in which electron spins are coupled together by the exchange interaction and all electrons on the Fermi surface contribute towards the wave phenomenon. The Larmor waves are associated with the precession of the individual spins in a magnetic field applied perpendicular to the surface of the sample. Under this condition, electrons at the surface experiencing the driving microwave fields will develop a net precessing magnetization transverse to the dc field. As the electrons move away from the surface on their cyclotron orbits, the transverse magnetization will continue to precess at the Larmor frequency determined by their g values. Electrons reaching the opposite side of the sample without scattering will have a transverse magnetization whose phase relative to the driving fields is given by

$$\phi=(\omega_0-\omega)L/v_H \tag{1}$$

where $\omega_0=g\mu_B H/\hbar$ is the Larmor frequency, ω is the driving frequency of the incident microwaves, L is the sample thickness, and v_H is the average drift velocity of the electrons along the field. Equation (1) gives the phase for all electrons on a thin slice cut through the Fermi surface perpendicular to the field. The various slices making up the Fermi surface will each contribute to the propagation of magnetization, but the phases in general will differ from slice to slice due to variations in v_H (and also ω_0 if g anisotropy is present). The net signal is obtained by summing the contributions from the various slices. This gives a very weak signal which is due to those electrons on orbits for which the phase is extremal, for only such orbits will have in their proximity many electrons which can arrive at the receive cavity with approximately the same phase. For a spherical Fermi surface such an extremal orbit corresponds to the limiting point where electrons travel almost parallel to the applied field. The Larmor-wave signal consists of a linear oscillation in the phase of the transmitted microwave field which occurs as the magnetic field is swept [see Eq. (1)].

One very useful feature of the Larmor waves is that they give information about a particular group of electrons on the Fermi surface rather than information which has been averaged over the entire electron distribution. However, as a consequence of the small number of electrons that contribute to these signals, the Larmor waves are exceedingly weak and have only been detected with the use of special techniques to enhance their strength. It was first noted by Janossy and Monod[5] that the coupling between the incident microwave fields and the electron

spins in a metal could be strongly enhanced by applying a thin ferromagnetic layer to the surface of the metal. By applying such ferromagnetic layers to both surfaces of a sample, it is possible to enhance the Larmor-wave spectra by a factor of several hundred to a few thousand,[6] enabling their easy detection with a conventional transmission spectrometer. For the original observations the ferromagnetic layers consisted of a few hundred angstroms of either evaporated permalloy or an amorphous alloy of cobalt and phosphorus.[7]

Surprisingly, very little has been published on the experimental observation of Larmor waves in metals. All that exists in the literature are the original observations by Janossy and Monod[1] in Cu and gold, and a more extensive later report by Janossy[6] on Cu, gold, and tungsten. These two publications concentrate on single crystals of Cu oriented with either the ⟨100⟩ or ⟨110⟩ crystal axes perpendicular to the plane of the specimen. All these observations were carried out at X-band frequencies (9 GHz). The motivation for the present study at 80 GHz was an initial observation at 80 GHz of two Cu samples provided by Janossy from the original ones which had been studied at 9 GHz. As reported recently by us,[8] the higher-frequency observations were quite different from the original ones, with the amplitude and period of the Larmor waves showing a much stronger temperature dependence. Further study on those samples showed that they were no longer single crystals, so a new set of single-crystal plates was prepared for the study reported here.

The theoretical nature of Larmor waves was studied by Montgomery and Walker.[9] Their theory includes not only the effects of Fermi-surface anisotropy and g-tensor anisotropy but also takes into account Fermi-liquid interactions, which arise from the quantum-mechanical exchange interaction between the electrons. The presence of the Fermi-liquid effects modifies the spacing of the phase oscillation such that their period in magnetic field becomes

$$\Delta H=\frac{2\pi\hbar v_H(1+B_0)}{g\mu_B L}=\frac{2\mu\hbar v_H}{g_{\rm SP}\mu_B L} \tag{2}$$

where B_0 is the first spin-dependent Landau Fermi-liquid parameter.[4] B_0 represents the contribution of an effective exchange field due to neighboring spins which must be added to the externally applied magnetic field. The free-electron result is obtained by letting B_0 go to zero. As indicated in Eq. (2), the factor $1+B_0$ can be combined with the usual g value (determined from the CESR) to obtain the "single-particle" g value:

$$g_{\rm SP}=\frac{g}{1+B_0}\ .$$

$g_{\rm SP}$, which can be measured by the de Haas–van Alphen (dHvA) Effect, determines the precessional frequency of a single spin in an applied external field when all the other spins are frozen in their equilibrium positions. This modification of the g value represents another method to take into account the exchange field due to neighboring spins. Under certain simplifying conditions and Fermi-surface geometries, Montgomery and Walker were able to calculate Larmor-wave line shapes. Unfortunately, none of the computations appears to provide a complete, realistic description of what has been seen in our Cu specimens.

II. EXPERIMENTAL TECHNIQUE

A. Sample preparation

The samples consist of thin plates of high-purity, single-crystal Cu with the principle axes ⟨100⟩, ⟨110⟩, and ⟨111⟩ oriented perpendicular to the plane of the specimen. The samples were aligned to within 1° or better of the desired direction using back-Laue x-ray reflection. Table I lists the individual samples studied and their thicknesses at low temperature. This includes one polycrystalline sample run for comparison purposes. The thicknesses were measured at room temperature with a micrometer and then corrected for a 0.3% thermal contraction to liquid-helium temperatures.[10] On several occasions thinner samples were prepared from thicker ones after completing the study with the larger dimension.

Initially, relatively thick slices were cut from a large single crystal of Cu using a low-speed diamond saw. These were next lapped to approximately the desired thickness and then etched in a dilute solution of nitric acid to remove the damaged layer at each surface. To maximize the low-temperature electrical conductivity, the samples were annealed at 900 °C in air at a pressure of 10^{-4} Torr.[11] This produced a residual resistance ratio (RRR), measured between 295 and 4.2 K, of 6800 for the bulk material. A reduced RRR was observed in the thinner samples due to an increased surface scattering of the conduction electrons.

To enhance the electromagnetic coupling to the electron spins, ferromagnetic layers were deposited on both surfaces. For all samples this was accomplished by electroplating an amorphous alloy of cobalt and phosphorus (Co-P) as described in Ref. 7. The thickness of the film is estimated to be of the order of 1000 Å, much less than the microwave skin depth of the Co-P. In some cases samples were run both with and without the ferromagnetic coating so that the Larmor-wave signals could be compared with the underlying Gantmakher-Kaner oscilla-

TABLE I. Cu samples used in the study of Larmor waves.

Orientation	⟨100⟩	⟨110⟩	⟨111⟩	Polycrystalline
Thickness	1060±5	623±5	691±5	212±3
(μm)	824±5	441±3	542±4	
	722±5	333±3	418±3	
	621±4	294±6	292±3	
	513±5	240±3	165±3	
	411±3	168±3	62±4	
	312±3	136±5	48±2	
	294±5	91±3		
	211±3	60±5		
	164±5			
	156±3			

tions[12] (GKO), which are due to the orbital motion of the conduction electrons in the applied field and are readily visible in the unplated specimens.

B. Microwave spectrometer

The 80-GHz transmission spectrometer has been described in detail elsewhere.[13] The sample is clamped between the two microwave cavities with indium gaskets on both sides of the sample to prevent the accidental leakage of microwaves around the specimen. The two rectangular cavities are aligned parallel with each other and used in the TE_{101} resonant mode. As a consequence, the conduction electrons on one side of the sample are driven by a *linearly polarized* rf magnetic field (parallel to the surface and perpendicular to the applied dc magnetic field), and on the other side of the sample the receive cavity responds to the linearly polarized component of the transmitted microwave field having the same orientation as the driving fields.

The microwave detector is an InSb bolometer operating at 4.2 K in a hot-electron mode. The bolometer is used as a microwave mixer, being biased by a small fraction of the microwave power which is incident on the transmit cavity. The detected signal is thus proportional to the cosine of the phase difference between the transmitted microwave field and that of the microwave reference. The sensitivity of the detector is approximately 10^{-21} W. A room-temperature Schottky microwave mixer diode is used to monitor the microwave power reflected from the transmit cavity. This allows one to monitor the ferromagnetic resonance (FMR) from the Co-P layer on one surface of the specimen.

The sample and cavities are situated at the center of a superconducting solenoid (60 kG capacity) inside of a vacuum can surrounded by liquid helium. Helium exchange gas in the can allows thermal contact with the helium bath. With the use of a heater and thermistor thermometer attached to the cavities, the temperature of the sample can be regulated and measured to within ± 0.2 K over the temperature range 4–40 K.

III. OBSERVATIONS

In this section we display examples of data for samples of varying thickness with the magnetic field aligned with the three principal axes. In addition to the Larmor-wave (LW) oscillations, GKO's can also occur (especially for the thinner samples). As the present theory is not able to account for the line shape of the data, we concentrate on the period of the oscillations in the magnetic field. According to Eq. (2) the product of the period and the sample thickness, ΔHL, should be the same for all samples with a fixed orientation, and this we call the "normalized period" (NP).[6] The NP is calculated only in regions where the oscillation period is constant over a range of several kG. This specifically excludes magnetic fields in the vicinity of the Cu CESR and the Co-P FMR, where the phase of the transmitted signal oscillates more rapidly. The LW oscillations have been divided into two classes: the "low-field" oscillations and the "high-field" oscillations depending on whether they occur at magnetic fields less than or larger than that of the Cu CESR, respectively. As will be seen, these two classes of oscillations can have amplitudes and temperature dependencies which are rather different from each other. It should also be noted that the FMR of the Co-P has a strong loading effect on both cavities, reducing the Q's and coupling to the two cavities. Consequently, in the vicinity of the FMR both the transmitted and reflected signals are reduced considerably in amplitude from what would be seen without this loading effect.

A. $\mathbf{H} \| \langle 100 \rangle$

In this geometry Cu samples whose thicknesses range from 1060 to 156 μm have been studied. Figure 1 shows both the transmission and reflection spectrum for the thickest sample at a temperature of 4.2 K. The transmission spectrum, shown in 1(a), displays LW oscillations in only two small regions of magnetic field: the low-field oscillations centered at 20 kG and the high-field oscillations centered at 45 kG. No GKO signals are present and neither is the Cu CESR, which occurs at 27.5 kG for this frequency. The more slowly varying baseline is due to an unusually large amount of accidental microwave leakage between the two cavities for this particular sample. Within experimental uncertainty, the NP of the low-field oscillations (37.5 ± 0.6 G cm) is equal to the NP of the high-field oscillations (36.5 ± 0.6 G cm). This is very close to the NP = 38 G cm observed by Janossy at 9 GHz. The temperature dependence of the LW for this thickness was not studied as the signal was too weak.

The reflection spectrum from the transmit cavity, shown in Fig. 1(b), displays three separate peaks, labeled as A, B, and C, which are associated with the Co-P layer. The largest peak, A, corresponds to the uniform FMR mode. This is also seen in the microwave leakage superimposed on the transmission spectrum of Fig. 1(a), where it has been labeled as feature D. This resonance in the ferromagnetic layer is shifted by the demagnetization field,[14] $4\pi M$, where M is the dc magnetization of the Co-P. The FMR generally occurs at fields of 43 ± 3 kG, with variations due to small differences in the Co-P magnetization from sample to sample. The peaks B and C are identified as bulk and surface spin-wave modes[15] of the ferromagnet, respectively. Note that the high-field LW's are most closely associated with the surface spin-wave mode.

As the sample thickness is reduced, the transmission signal rapidly grows larger due to the increasing number of electrons which cross the sample without scattering. In addition, the magnetic field range over which the LW's are present increases. The low-field oscillations remain centered at 20 kG (for which we have no simple explanation), and the high-field oscillations remain strongest in the vicinity of the FMR. For the thinner samples we often calculate the NP of the high-field oscillations at magnetic fields lying between the Cu CESR and the Co-P FMR, where the period appears to be most uniform. Figure 2 displays that portion of the transmission spectrum extending from 17 to 49 kG for a 722-μm-thick specimen at 4.2 K. In addition to the low-field and high-

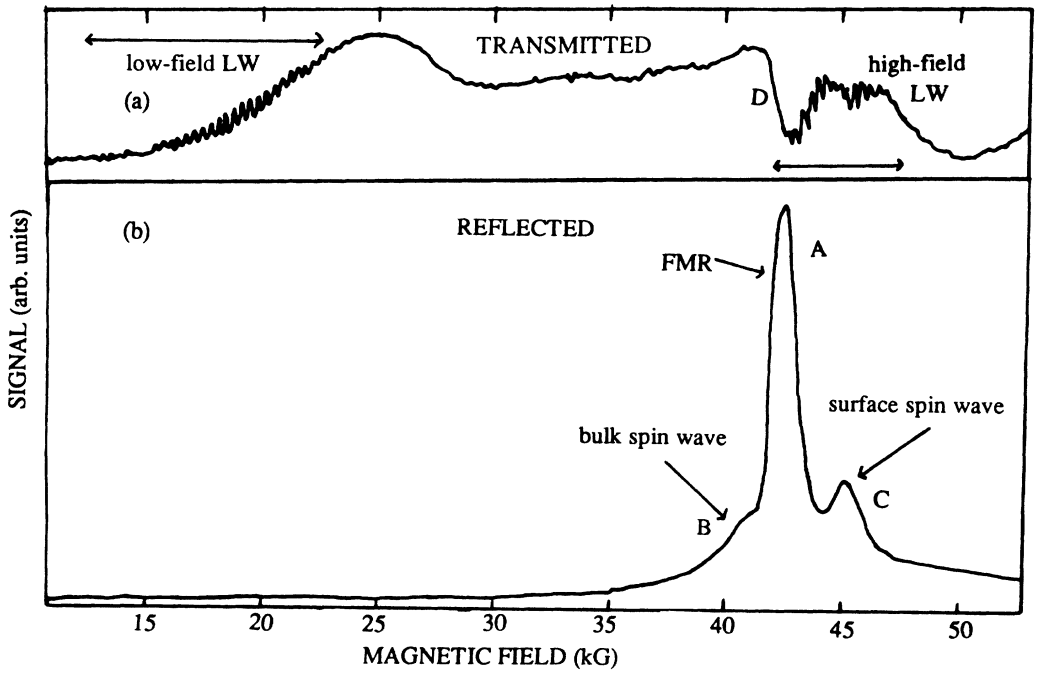

FIG. 1. The (a) transmission and (b) reflection spectra observed in a ⟨100⟩ Cu specimen of thickness 1060 μm at 4.2 K.

field LW's indicated in the figure, the Cu CESR is also clearly seen. As the temperature was increased to 16 K, the LW weakened, due to increasing electron-phonon scattering, while the CESR signal *narrowed* in width with the amplitude remaining virtually the same. This observation on the CESR is in agreement with previous studies done on unplated Cu,[16] and is due to the presence of g anisotropy[17] on the Fermi surface coupled with motional narrowing.[18] Once again, for this sample the NP for oscillations on both sides of the CESR did not show an appreciable temperature dependence.

When the thickness of the sample is further reduced, GKO signals appear in certain portions of the transmission spectrum. Figure 3 shows the transmission signal for a 411-μm-thick specimen at 4.2 K. In addition to the CESR and low-field LW signals, fine structure is observed at still lower fields in the range 5–13 kG. This fine structure is due to the third and fifth subharmonics of a certain class of GKO signal (extremal helical trajectory) as seen in unplated Cu specimens and described in detail in Ref. 12. The NP for the GKO signals seen in Fig. 3 is in exact agreement with that obtained with unplated samples. Another class of GKO signal seen in unplated samples for this geometry (arising from a cutoff of the topological effectiveness[12]) has a normalized period NP$=51.8\pm2$ G cm, which is sufficiently different from that of the LW as to be easily distinguished.

For the thinner specimens it is observed that the NP becomes different for the low-field and high-field oscillations. Furthermore, a corresponding temperature dependence is recorded as well, which is most prominent for the high-field LW. Figure 4 displays the temperature dependence of the NP for five different samples ranging in thickness from 824 to 156 μm. Also indicated is the temperature-independent value measured by Janossy at 9 GHz. As can be seen for the two thicker samples, the high-field and low-field LW oscillations have approximately the same NP, which is relatively temperature independent and close to the 9-GHz value. On the other hand, the three thinnest samples display a distinct varia-

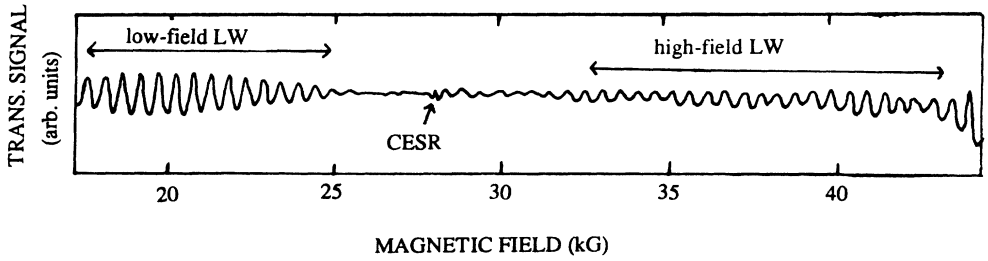

FIG. 2. The transmission signal for a ⟨100⟩ Cu sample of thickness 722 μm at 4.2 K.

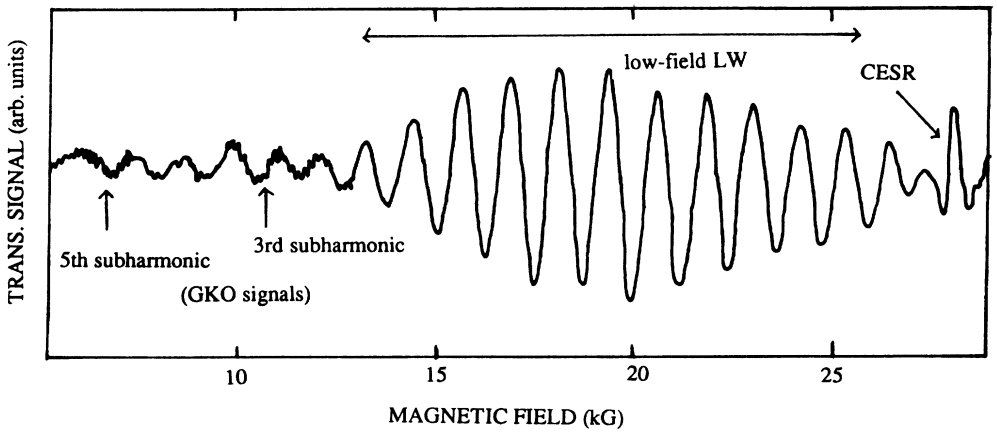

FIG. 3. The transmission spectrum for a ⟨100⟩ Cu sample of thickness 411 μm at 4.2 K.

tion with temperature. The low-field oscillations are least affected by temperature and lie closest to the 9-GHz measurement. The high-field oscillations have a NP that is several percent less and relatively temperature independent in the range 4–12 K, but which increases at higher temperature, approaching the value of the low-field oscillations (and the 9-GHz value) at temperatures around 18–20 K. This temperature variation at 80 GHz may reflect a dependence on the quantity $\omega\tau$, which, according to dc electrical resistivity measurements, is also approximately constant over the temperature range 4–12 K. This possibility is also consistent with the smaller differences between the high-field and low-field NP seen in the thinnest samples, which would have a reduced $\omega\tau$ from increased surface scattering.

Because the temperature dependence of the NP is present only in the thinner samples, another mechanism which might play a role could be the contribution of two or more groups of electrons from different parts of the Fermi surface which individually would have somewhat different periods. For samples whose thickness is larger than the electron mean free path Λ (the thickest samples or thinner samples at elevated temperature where electron-phonon scattering makes a significant contribution), scattering events rapidly attenuate the strength of the signal. In such a sample, the signal would be dominated by just one class of extremal electrons—those having the largest value of v_H and traversing the sample most quickly. For situations in which $L < \Lambda$, however, it may be possible for another group of extremal electrons to make a significant contribution. Having a smaller value of v_H, this group of electrons would give rise to LW's with a smaller period ΔH [see Eq. (2)]. These characteristics are consistent with the general features seen in the thickness and temperature dependence displayed in Fig. 4. LW oscillations made up of a combination of signals of different frequencies should in general display a beating pattern. This is indeed observed to some extent in the high-field oscillations as illustrated in Fig. 5, where a clear amplitude modulation is visible over the magnetic field range 30–40 kG.

B. H‖⟨110⟩

In this geometry Cu samples whose thicknesses range from 623 to 60 μm have been studied. Figure 6 shows the transmission spectrum for the thickness sample at a temperature of 4.2 K. For this orientation the signal amplitude is quite asymmetric with respect to the CESR with the high-field oscillations being considerably stronger than the low-field oscillations. Only the high-field LW's are shown as the low-field ones are too weak to obtain much useful data. Also, the temperature dependence of the transmission spectrum was not studied for this sample. The NP of the high-field oscillations for this sample is 20.8±0.5 G cm. The NP of the GKO observed by Hsu and Dunifer[12] over this field range for unplated ⟨110⟩ Cu samples varied between 23 and 27 G cm. This is sufficiently close to that of the oscillations in Fig. 6 that some caution must be exercised to ensure that there are no complications from GKO present in the background. Referring to Fig. 8 of Ref. 12, it is seen that the GKO signals in this region have a magnetic field dependence to their amplitude which is rather different than that seen in Fig. 6. Two classes of GKO are superimposed, one having an amplitude which slowly decreases from 27 to 43 kG, and the other being a localized signal peaked at 35 kG. Furthermore, there is no beating pattern present in Fig. 6. Consequently, it appears quite certain that the observed oscillations are due to LW only.

Figure 7 displays the transmission signal for a 441-μm-thick sample at 4.2 K. Figure 7(a) presents the low-field data for $H < 30$ kG. GKO signals (due to an extremal helical trajectory[12]) are present at the lowest magnetic fields. The NP of 10.6±0.3 G cm for these oscillations agrees with the value obtained by Hsu and Dunifer:[12] 10.7±0.3 G cm. The low-field LW's are indicated in the figure and have a uniform period over the range 21–26 kG with a NP=17 G cm. GKO oscillations at these magnetic fields have a NP=35 G cm, twice as large. Figure 7(b) shows high-field oscillations for $H > 30$ kG. The high-field LW's have a uniform period, NP =21.2±0.3 G cm, over a range of 15 kG. This is in con-

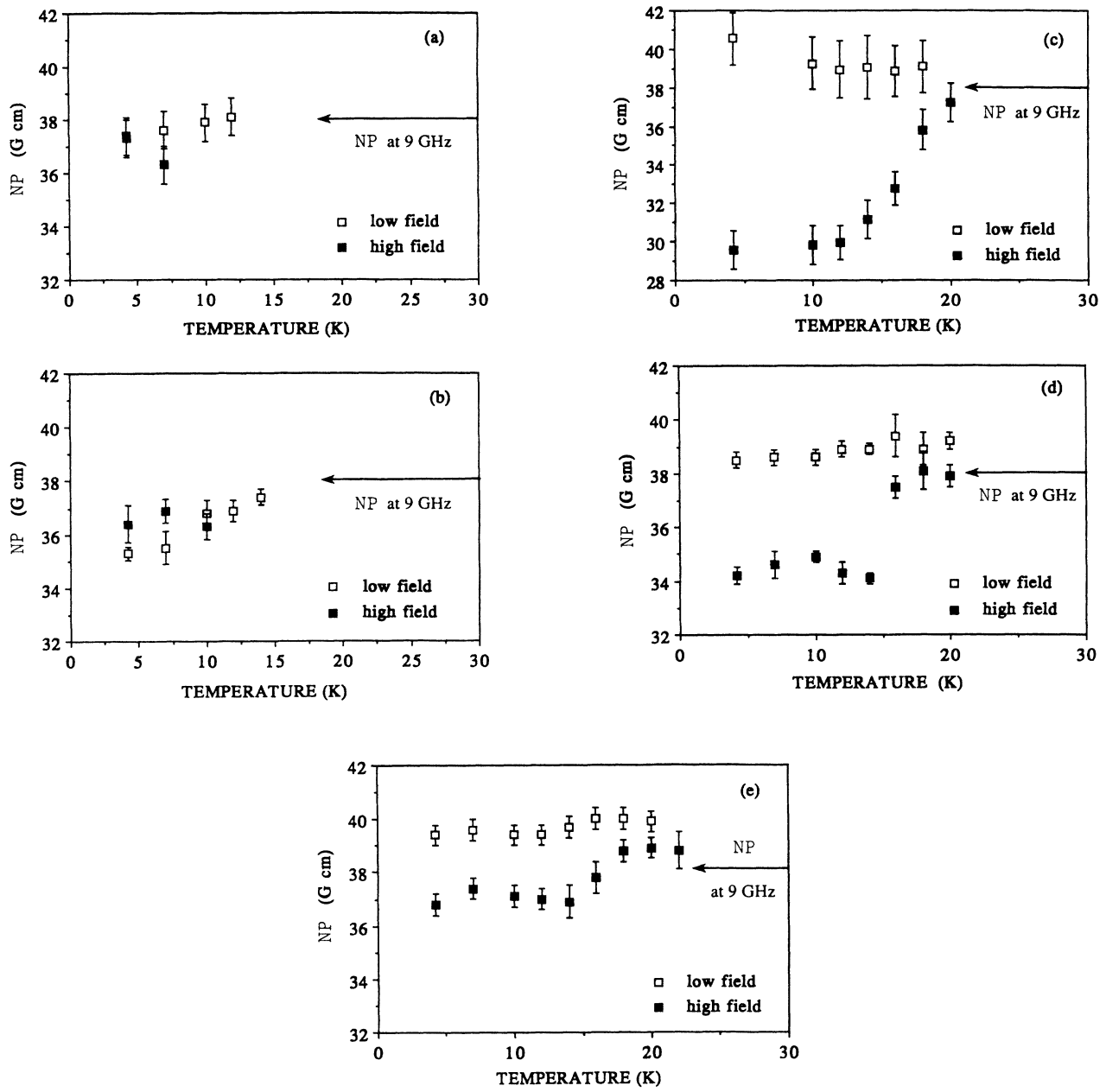

FIG. 4. The temperature dependence of the NP for ⟨100⟩ Cu samples of different thicknesses. The horizontal arrow indicates the temperature-independent value measured at 9 GHz. The various thicknesses are (a) 824 μm, (b) 621 μm, (c) 294 μm, (d) 211 μm, (e) 156 μm. [The data in (c) are obtained from one of Jánossy's original samples, and although mostly ⟨100⟩ orientation, may contain small crystallites of other orientations.]

trast to the GKO in unplated samples whose period varies by more than 15% over the same magnetic field range. Once again, the amplitude of the high-field LW dominates that of the low-field LW: by approximately a factor of 15 for this sample. Transmission spectra were studied up to a temperature of 13 K for this thickness.

As was done for the previous geometry, Fig. 8 displays the temperature dependence of the NP for ⟨110⟩ samples having different thicknesses. The 441-μm sample, shown in 8(a), displays essentially no temperature dependence; however, the high-field LW's have a NP approximately 25% *larger* than that of the low-field oscillations. The thinner samples do show a dependence on temperature, and presumably so would the 441-μm sample if the LW's could have been followed to somewhat higher temperatures before they faded away. The general behavior seen for the two thinnest samples, Figs. 8(c) and 8(d), is that the low-field LW's have an almost constant period, displaying, perhaps, a small increase at the highest temperatures. The high-field LW's have a NP that is essen-

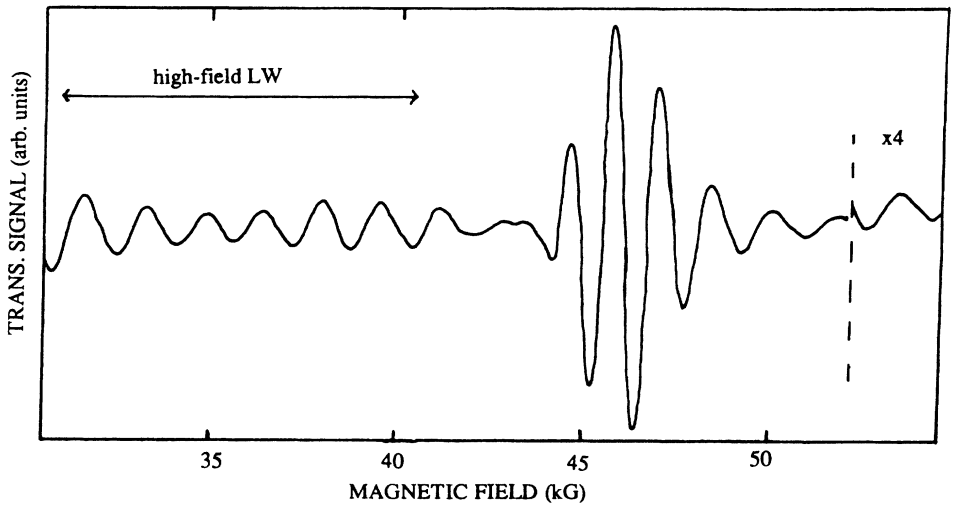

FIG. 5. The transmission signal for a ⟨100⟩ Cu specimen of thickness 211 μm at 14 K. Note the signal enhancement near 46 kG due to the Co-P FMR and the 4× increase in gain at 52 kG.

tially constant from 4–12 K, decreasing from 12–16 K, and becoming equal to that of the low-field LW for $T \geq 16$ K. This is the same type of behavior observed for ⟨100⟩ samples except that in this case the high-field LW's have a NP at low temperature which is *larger than* instead of less than that of the low-field ones. The values obtained for the NP for ⟨110⟩ Cu samples studied by Janossy at 9 GHz at 4.2 K are scattered between 18 and 22 G cm, covering approximately the range of our measurements.

C. H∥⟨111⟩

In this geometry Cu samples whose thicknesses range from 691 to 48 μm have been studied. Figure 9 shows the transmission spectrum for the thickest sample at a temperature 4.2 K. The high-field and low-field LW's and the CESR are indicated. The profile of this trace is similar to that obtained for the thicker ⟨110⟩ samples, where the high-field LW's are considerably more intense than the low-field ones. The low-field LW's reach maximum intensity at about 24 kG and have a uniform period extending over a range of about 5 kG. The high-field LW's have a uniform period over a range of almost 10 kG, but display a sudden change in their characteristics at magnetic fields in the vicinity of 37 kG. This is due to interference of the LW with exceptionally strong GKO, which occurs for $H \geq 36$ kG in the ⟨111⟩ geometry.[12]

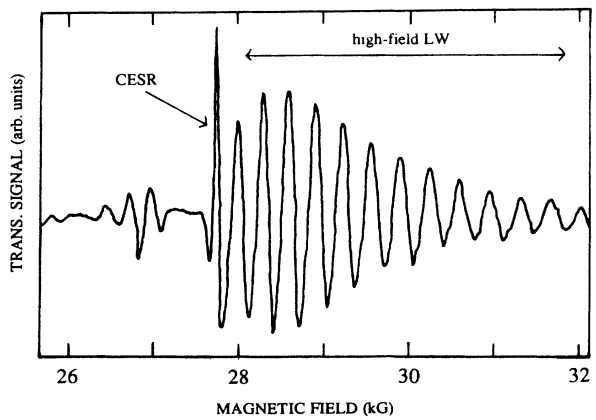

FIG. 6. The transmission spectrum for a ⟨110⟩ Cu sample of thickness 623 μm at 4.2 K.

This interference is further illustrated in Fig. 10 for a 418-μm-thick sample at 4.2 K. The dotted curve in the figure displays the modulus of the GKO signal recorded by Hsu and Dunifer[12] in an unplated Cu sample of comparable thickness. It is very clear from the figure that the beating pattern occurs over exactly the same range of magnetic field in which the GKO's have a significant amplitude. As the temperature is raised, electron-phonon scattering reduces the amplitude of the GKO more rapidly than that of the LW signals. By 18 K the GKO have essentially vanished for the 418-μm sample, allowing the high-field LW to be followed over a range of 20 kG as shown in Fig. 11. As the temperature is raised and the beating pattern disappears, the average NP of the oscillations for $H \geq 37$ kG decreases from 39 G cm (at 4.2 K) to 33 G cm (at 18 K), the same as that of the LW for $H < 37$ kG. Figure 12 shows the low-field transmission signal in this sample at 4.2 K. As can be seen, the low-field LW's occupy only a limited region of the spectrum with GKO (of the extremal-helicial-trajectory type[12]) dominating the remainder.

Figure 13 plots the temperature dependence of the NP of ⟨111⟩ samples of different thicknesses. The general trend present in the figure is that the NP of the *high-field* LW is relatively temperature independent (NP=33±1 G cm), while the NP of the low-field oscillations has some temperature dependence. The low-field LW's have a NP

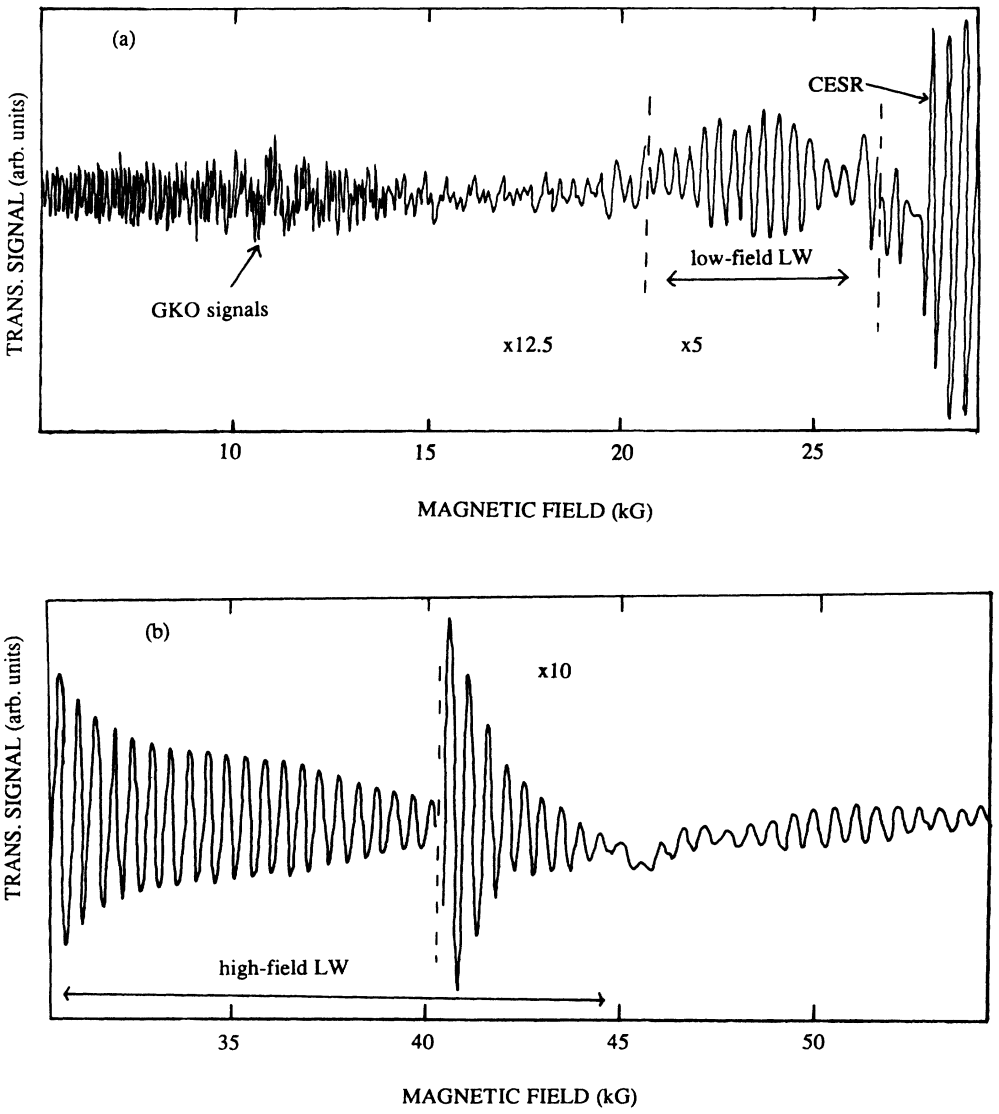

FIG. 7. The transmission signal for a ⟨110⟩ Cu sample of thickness 441 μm at 4.2 K. (a) Low-field regime. Note the change of gain near 21 and 27 kG. Highest gain is at the lowest fields; lowest gain is at the highest fields. (b) High-field regime. Note the change of gain near 40 kG.

which is constant and less than that of the high-field ones for temperatures less than 10 K, but which increases at higher temperature and approaches that of the high-field LW at temperatures around 15 K. This is similar to the behavior exhibited by the ⟨100⟩ and ⟨110⟩ samples except that the roles of the high-field and low-field LW's are interchanged. When the same plots are made for still thinner samples, there is more scatter in the data and less evidence for any particular pattern present. There exists no study of LW's for ⟨111⟩ samples at 9 GHz with which the above data can be compared. The NP of the GKO observed by Hsu and Dunifer[12] in unplated Cu samples for this crystal orientation was 44 G cm in the vicinity of the high-field LW and 25.4 G cm in the vicinity of the low-field LW.

D. Polycrystalline sample

A polycrystalline sample of thickness 212 μm and RRR = 1400 was studied for comparison purposes with the single-crystal specimens. Viewed under an optical microscope, the surfaces displayed individual crystallites having typical dimensions of 0.6 mm. Approximately 25 of the individual crystallites were directly exposed to the microwave fields of the transmit cavity. The transmission spectrum was studied between 4.2 and 20 K.

At 4.2 K complex GKO signals appeared at the lowest and highest fields. LW oscillations, along with the CESR signal, are found for 20 kG $\leq H \leq$ 40 kG. Interestingly, the LW's showed *no significant temperature dependence* to their period. The NP for the low-field LW was 33±2

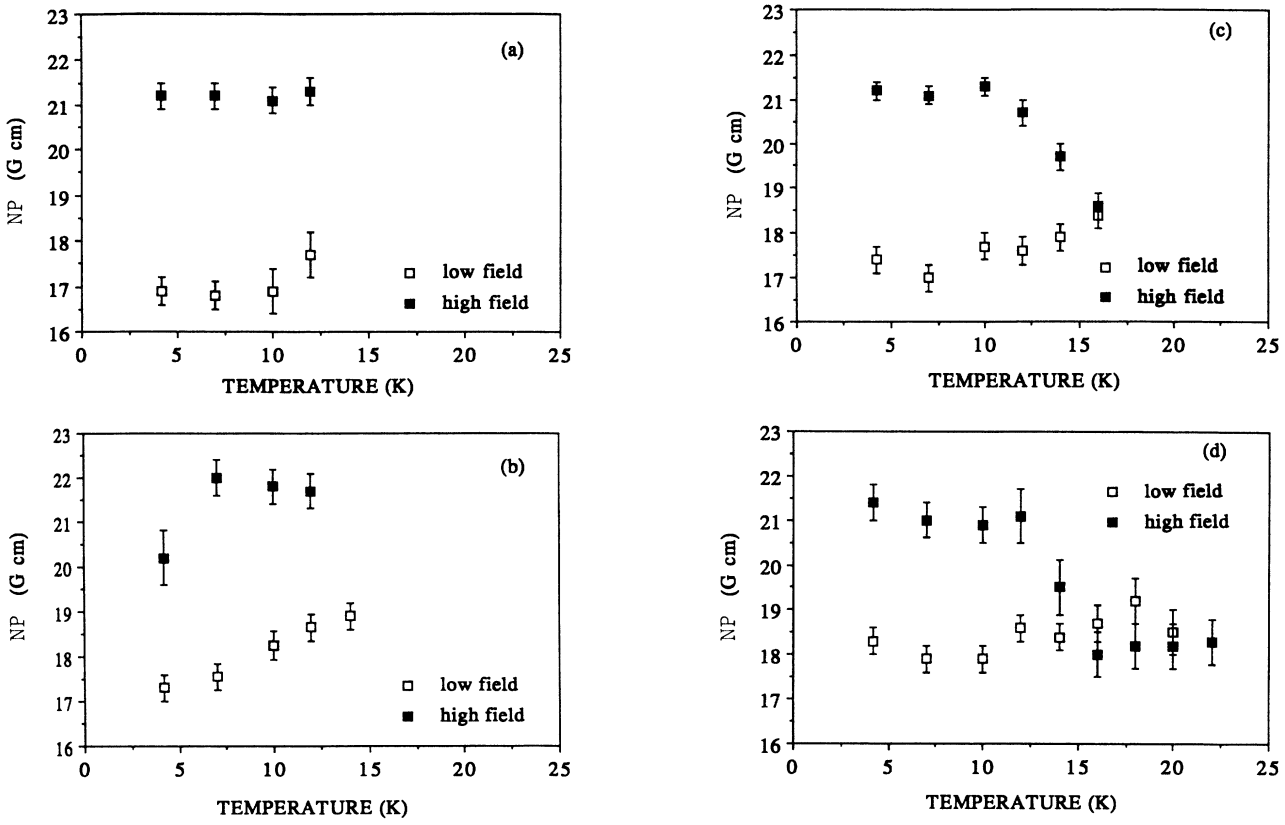

FIG. 8. The temperature dependence of the NP for ⟨110⟩ Cu samples of different thicknesses: (a) 441 μm, (b) 333 μm, (c) 240 μm, (d) 168 μm.

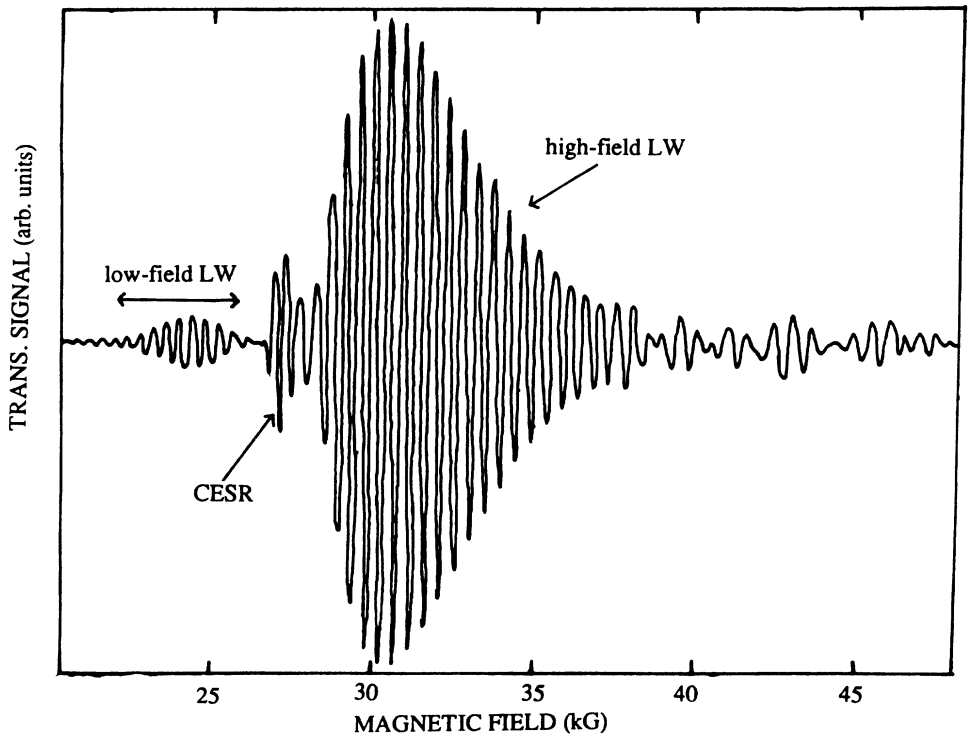

FIG. 9. The transmission signal for a ⟨111⟩ Cu sample of thickness 691 μm at 4.2 K.

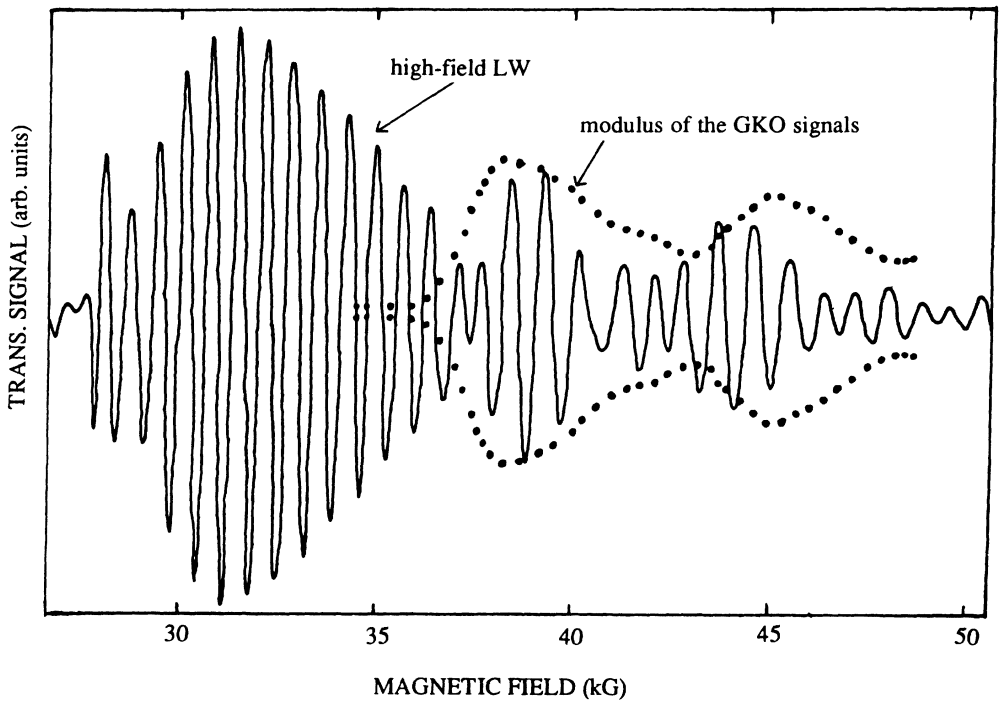

FIG. 10. The high-field transmission signal for a ⟨111⟩ Cu sample of thickness 418 μm at 4.2 K. The dotted curve displays the envelope of the GKO signal observed in an unplated Cu sample of comparable thickness for this orientation.

G cm; while the NP for the high-field LW was 31±2 G cm. These periods are closest to those displayed by single crystals of ⟨111⟩ orientation, indicating that there may be a preferred ⟨111⟩ orientation within the polycrystalline specimen.

IV. ANALYSIS AND DISCUSSION

As shown by Montgomery and Walker,[9] the magnetic field dependence of the LW amplitude becomes difficult to calculate for anisotropic Fermi surfaces, such as Cu,

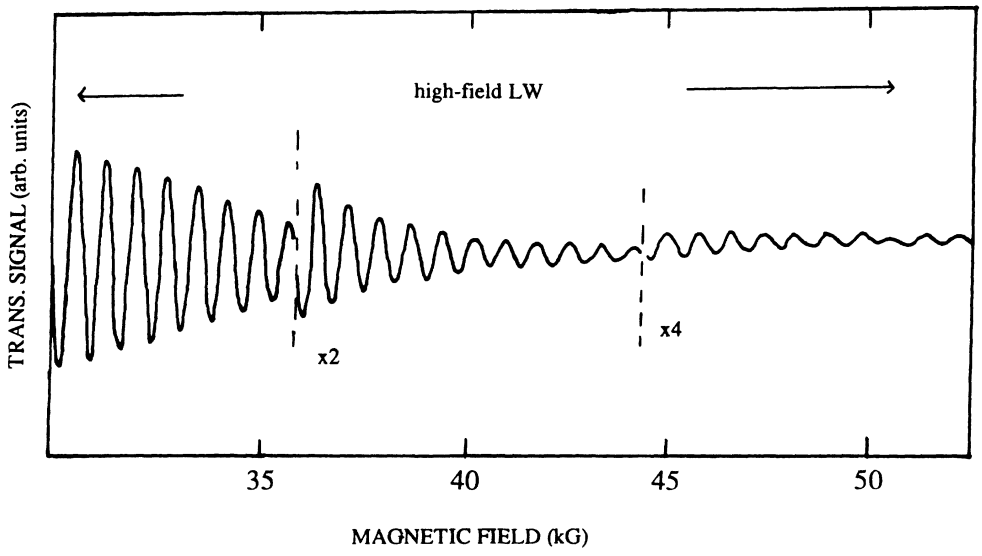

FIG. 11. The high-field LW for a ⟨111⟩ Cu sample of thickness 418 μm at 18 K. Note the doubling of the gain at magnetic fields near 36 and 44 kG.

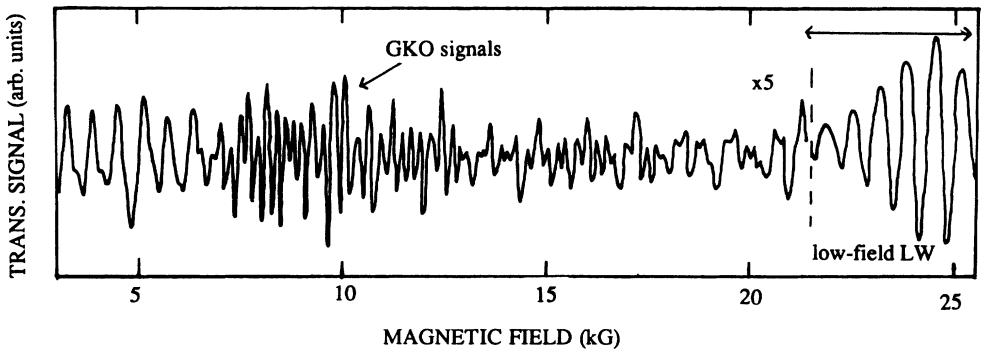

FIG. 12. The low-field transmission spectrum for a ⟨111⟩ Cu sample of thickness 418 μm at 4.2 K. Note the change in gain by a factor of 5 at a magnetic field near 22 kG.

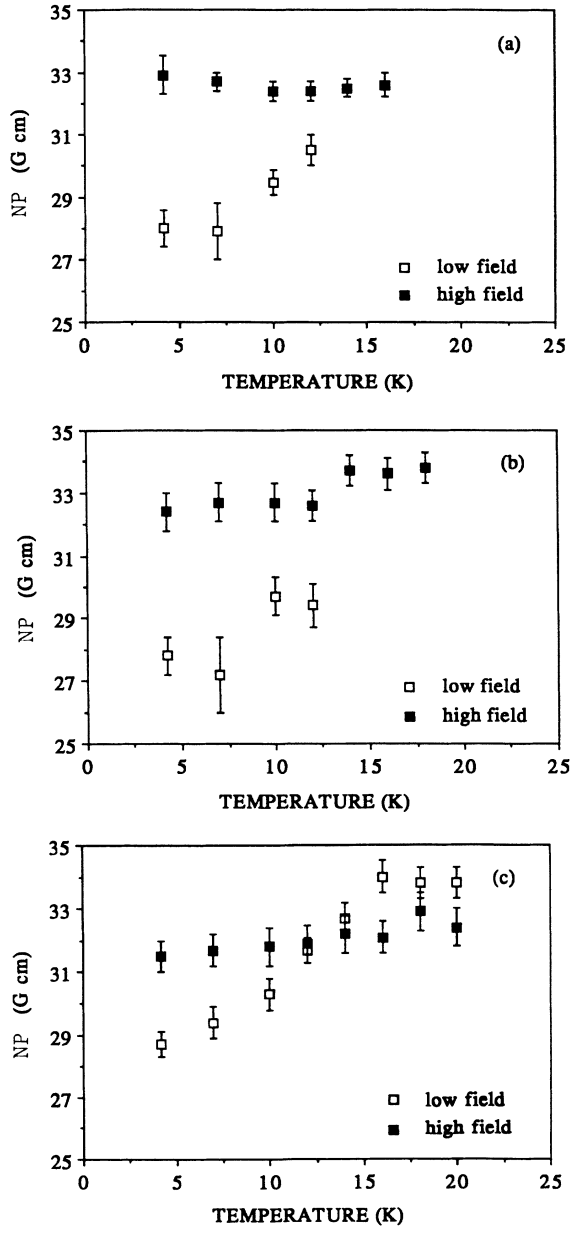

FIG. 13. The temperature dependence of the NP for ⟨111⟩ Cu samples of different thicknesses: (a) 691 μm, (b) 542 μm, (c) 418 μm.

especially in the presence of a significant exchange interaction. On the other hand, Eq. (2) for the normalized period is expected to be quite generally valid.[9] We will use this equation to calculate the NP for the known Fermi surface of Cu and compare the results with the experimentally determined periods for the three crystal orientations studied.

LW's arise from those groups of electrons on the Fermi surface whose phase passes through an extremum. From Eq. (2) it is seen that this requires an extremum in the quantity v_H/g_{SP}. Presumably for a material with g anisotropy on the Fermi surface, the extremal quantity should actually be $v_H/\langle g_{SP}\rangle$, where $\langle g_{SP}\rangle$ is the time-averaged g value for one complete orbit of an electron around the Fermi surface. v_H has already been defined as the average drift velocity of the electron along the field.

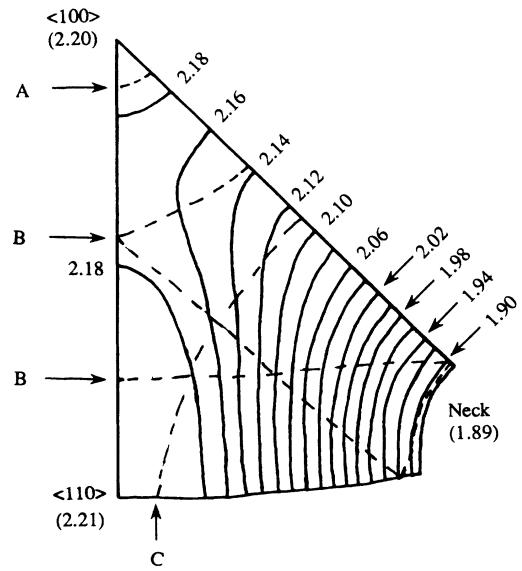

FIG. 14. A contour map showing the variation of g_{SP} on the Fermi surface of Cu. The dashed curves show the approximate orbits which are excepted to produce the dominant LW signals: *A*, $\mathbf{H}\|\langle 100\rangle$; *B*, $\mathbf{H}\|\langle 110\rangle$; and *C*, $\mathbf{H}\|\langle 111\rangle$. Note that orbit *B* has four separate segments.

g_{SP} has been measured for Cu by Randles[17] using the dHvA effect, and Fig. 14 displays its variation on the Fermi surface in the form of a contour map. Only $\frac{1}{48}$ of the Fermi surface has been shown as the remainder can be generated from symmetry. The characteristics displayed in the figure arise from both the exchange interaction and spin-orbit coupling to the lattice potential. The total variation of g_{SP} is only 16%, which is considerably smaller than that expected for v_H. Consequently, LW signals will arise, to a good approximation, from those orbits for which the quantity v_H is extremal.

v_H has been previously computed[12,16,19] using Halse's dHvA data[20] on the Fermi surface of Cu. This is displayed in Fig. 15 for the three geometries we have studied. k_H is the component of the electron's wave vector parallel to the applied field, and the normalizing quantity k_{FE} represents the radius of the Fermi surface for a free-electron gas having the same density as the conduction electrons in Cu. Arrows on the figure correspond to regions where v_H has an extremum or is approximately constant, both of which can give rise to LW signals.

For the ⟨100⟩ geometry, shown in Fig. 15(a), three different values of k_H have been indicated which might produce LW's. The value of v_H associated with k_3 is about 3 times smaller than that of the other two wave vectors. Because these electrons are much more likely to suffer a scattering event in crossing the sample, it is not likely that they will generate observable LW's except in the thinnest samples. The values of v_H lying between k_1 and k_2 vary by only about 4%. Consequently, one might expect a significant fraction of the electrons lying between these two values could participate in the observed LW signal. For comparison with the experimental data, we have calculated in Table II, using Eq. (2), the NP expected for those electrons having $k_H = k_1$. For the indicated value of k_1, we have listed in the table the associated values of v_H and $\langle g_{SP} \rangle$ used in the equation. The value given for $\langle g_{SP} \rangle$ is not an exact value, but rather a "best estimate" obtained by averaging the g value over the required orbit with the aid of the contour map in Fig. 14 and a tracing of the orbit on a three-dimensional model of the Cu Fermi surface. The approximate location of this orbit on the contour map is given by the dashed curve labeled *A*.

The calculated value NP = 35.8±0.7 G cm can be compared with the experimental values displayed in Fig. 4. For the two thickest samples, which do not show much temperature dependence, the NP's are just a little larger than the calculated value. For the 211-μm sample, which has the largest temperature dependence, the calculated value is close to that observed in the high-temperature limit where the low-field and high-field values are approaching each other and that measured at 9 GHz. Because of this, we list for the experimental NP in Table II the value 38.3±0.7 G cm, which is obtained by averaging the *high-temperature* results for all the ⟨100⟩ samples. This number is about 7% larger than the calculated value and somewhat too large to allow overlap of the two sets of error bars. Recalculating the NP using the electrons at $k_H = k_2$ gives NP = 34.7 G cm, which agrees even less well with the experimental data.

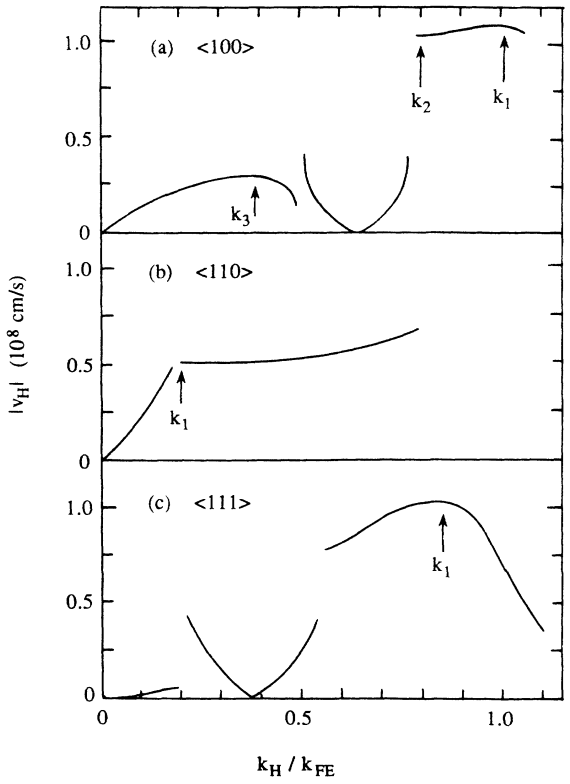

FIG. 15. A plot of v_H vs the ratio k_H/k_{FE} for Cu. (a) $\mathbf{H}\|\langle 100\rangle$, (b) $\mathbf{H}\|\langle 110\rangle$, (c) $\mathbf{H}\|\langle 111\rangle$.

For the ⟨110⟩ geometry, shown in Fig. 15(b), there is a range of wave vectors, $0.2 \leq k_H/k_{FE} \leq 0.35$, over which v_H is essentially constant and from which LW's might arise. The specific orbit which plays the dominant role

TABLE II. Comparison of the experimental LW period with values calculated from the Fermi-surface geometry.

Crystal orientation	⟨100⟩	⟨110⟩	⟨111⟩
k_1/k_{FE}	1.01	0.20	0.87
v_H (10^8 cm/s)	1.096±0.005	0.488±0.005	0.99±0.01
$\langle g_{SP} \rangle$	2.19±0.02	2.02±0.04	2.16±0.04
NP_{calc} (G cm)	35.8±0.7	17.2±0.5	32.8±0.8
NP_{expt} (G cm)	38.3±0.7	17.8±0.4	32.9±0.7

may be determined by where $\langle g_{SP} \rangle$ has an extremum in this vicinity. Guessing that this orbit, labeled with $k_H = k_1$, might be the one in which the electron just skims by the necks on the Fermi surface, we calculate the NP for this orbit in Table II in the same manner as was done for the $\langle 100 \rangle$ geometry. The approximate location of this orbit on the contour map is given by the dashed curve labeled B in Fig. 14. The calculated value NP$=17.2\pm0.5$ G cm is to be compared with the experimental data in Fig. 8. Once again, agreement is best at high temperatures, where the low-field and high-field periods merge together. The experimental value listed in Table II, NP$=17.8\pm0.4$ G cm, is the high-temperature average for all $\langle 110 \rangle$ samples. This agrees well with the calculated value above.

For the $\langle 111 \rangle$ geometry, shown in Fig. 15(c), there is only one wave vector k_1 at which v_H has an extremum. The NP of the LW for electrons in this orbit is calculated in Table II as before. The approximate location of this orbit on the contour map is given by the dashed curve labeled C. The calculated value, NP$=32.8\pm0.8$ G cm, is compared with the experimental data in Fig. 13. As before, the agreement is best at high temperature, where the average value for all $\langle 111 \rangle$ samples, NP$=32.9\pm0.7$ G cm, is in almost perfect agreement with the calculated result. We thus find very good agreement between the calculated and high-temperature experimental NP for the $\langle 111 \rangle$ and $\langle 110 \rangle$ orientations, but somewhat poorer agreement for the $\langle 100 \rangle$ direction.

The other two features of interest in the experimental data are the asymmetry in the LW amplitude with respect to the CESR for the $\langle 110 \rangle$ and $\langle 111 \rangle$ samples and the variation of the NP with temperature seen for all three orientations. Montgomery and Walker[9] show how the asymmetry in amplitude can result from an exchange interaction between the electrons (B_0 having a nonzero value). From numerical computations for both a spherical and cylindrical Fermi surface, they show that a negative value of B_0 will enhance the amplitude of the high-field LW over that of the low-field ones. Using a value $B_0 = -0.285$ (appropriate for potassium metal), they find an enhancement factor of as much as several hundred. Previous studies on the temperature and frequency dependence of the Cu CESR (Refs. 16 and 18) indicate that B_0 for this metal is negative, but with a rather small magnitude: $B_0 \approx -0.01$. This number is consistent with the enhancement of LW's on the high-field side of the CESR and also with the enhancement factor of 3–10 seen in the $\langle 110 \rangle$ and $\langle 111 \rangle$ samples (assuming the enhancement is proportional to $|B_0|$). Why the enhancement is not seen for $\langle 100 \rangle$ oriented specimens is not clear without a more detailed calculation taking into account the actual Cu Fermi surface.

We are not able to interpret the variation of the LW period with temperature at this stage. No variation was observed[6] at 9 GHz, but it is clearly present for all three orientations studied at 80 GHz. The temperature dependence seen for the $\langle 100 \rangle$ orientation may be partly due to electrons in the vicinity of $k_H = k_2$ [Fig. 15(a)] making a larger contribution in thinner samples as discussed in Sec. III A. This, however, cannot be the complete explanation, as no temperature variation was recorded at 9 GHz while observing some of the *same* samples. The temperature dependence may be due to a combination of many-body effects and the detailed geometry of the Fermi surface of Cu. Under the condition $|\omega\tau B_0/(1+B_0)| \geq 1$, many-body effects become much more prominent,[9,18] than when $|\omega\tau B_0/(1+B_0)| \leq 1$. With the small magnitude of B_0 in Cu, it is very likely at 80 GHz that one passes from one regime to the other as the temperature is raised from 4 to 20 K. On the other hand, at 9 GHz it is not likely that $|\omega\tau B_0/(1+B_0)|$ will approach 1 at any temperature. What is needed at this point is a rigorous calculation of the LW spectra in Cu taking into account the proper geometry of the Fermi surface and allowing a nonzero exchange interaction. The results of such a calculation should enable a more quantitative interpretation of the experimental data presented here and, perhaps, an accurate determination of the parameter B_0.

We conclude with a final remark on the Cu CESR. Since the CESR arises from all the electrons on the Fermi surface, one would expect this signal in general to be much stronger than the LW signals. This is the case in Figs. 1–4 of Montgomery and Walker[9] in which they display the results of numerical calculations for several different situations. On the other hand, as seen in some of the experimental traces presented here, the CESR may be either weaker than the LW or absent altogether. A more exact calculation for Cu should show how this situation arises.

V. CONCLUSION

LW's at 80 GHz have been studied in Cu samples plated with thin ferromagnetic layers for three crystal orientations (and one polycrystalline specimen). The normalized periods obtained for these LW's showed a temperature dependence of varying degree for the three orientations, in contrast to what was observed in earlier studies at 9 GHz. Despite the temperature dependence, the *high-temperature* NP's are comparable to the theoretical predictions and consistent with the lower-frequency studies. The observed asymmetry in the LW amplitude with respect to the CESR, seen for $\langle 110 \rangle$ and $\langle 111 \rangle$ samples, may be due to a weak exchange interaction ($B_0 \approx -0.01$). The present theory of LW's should be reevaluated using a more realistic model for Cu.

ACKNOWLEDGMENTS

This research was supported in part by National Science Foundation Grant No. DMR-84-14488. The authors would like to thank A. Janossy (Central Research Institute for Physics, Budapest, Hungary) for his five-week visit to the Wayne State University campus and helpful discussions with him on the nature of Larmor waves. Single-crystal Cu specimens were provided by S. Schultz (University of California, San Diego, La Jolla, California). The authors are also indebted to C. Peters (Ford Motor Company, Dearborn, Michigan), whose assistance in orienting the Cu single crystals by back-Laue x-ray scattering is greatly appreciated.

[1]A. Janossy and P. Monod, Phys. Rev. Lett. **37**, 612 (1976).
[2]For a more thorough discussion of the microwave transmission technique see D. Pinkel, G. L. Dunifer, and S. Schultz, Phys. Rev. B **18**, 6658 (1978).
[3]S. Schultz, G. L. Dunifer, and C. Latham, Phys. Lett. **23**, 192 (1966).
[4]G. L. Dunifer, D. Pinkel, and S. Schultz, Phys. Rev. B **10**, 3159 (1974).
[5]A. Janossy and P. Monod, Solid State Commun. **18**, 203 (1976).
[6]A. Janossy, Phys. Rev. B **21**, 3793 (1980).
[7]*Amorphous Magnetism*, edited by H. O. Hooper and A. M. deGraaf (Plenum, New York, 1973).
[8]G. L. Dunifer, A. T. Wijeratne, A. Janossy, and H. Hurdequint, Bull. Am. Phys. Soc. **29**, 490 (1984).
[9]D. S. Montgomery and M. B. Walker, Phys. Rev. B **19**, 1566 (1979).
[10]A. Goldsmith, T. E. Waterman, and H. J. Hirschhorn, *Handbook of Thermophysical Properties of Solid Materials* (Macmillan, New York, 1961), Vol. I.
[11]J. J. Gniewek and A. F. Clark, J. Appl. Phys. **36**, 3358 (1965).
[12]T. M. Hsu and G. L. Dunifer, Phys. Rev. B **28**, 821 (1983).
[13]G. L. Dunifer and M. R. Pattison, Phys. Rev. B **14**, 945 (1976).
[14]C. Kittel, *Introduction to Solid State Physics*, 5th ed. (Wiley, New York, 1976).
[15]L. J. Maksymowicz and D. Sendorek, J. Magn. Magn. Mater. **37**, 177 (1983).
[16]T. M. Hsu, Ph.D. thesis, Wayne State University, 1978 (unpublished).
[17]D. R. Randles, Proc. R. Soc. London, Ser. A **331**, 85 (1972).
[18]D. R. Fredkin and R. Freedman, Phys. Rev. Lett. **29**, 1390 (1972).
[19]T. G. Phillips, G. A. Baraff, and P. H. Schmidt, Phys. Rev. B **5**, 1283 (1972).
[20]M. R. Halse, Philos. Trans. R. Soc. London, Ser. A **265**, 507 (1969).